Journal of Radiation Research, 2012, 53, 840–853
doi: 10.1093/jrr/rrs060

5-AED enhances survival of irradiated mice in a G-CSF-dependent manner, stimulates innate immune cell function, reduces radiation-induced DNA damage and induces genes that modulate cell cycle progression and apoptosis

Marcy B. GRACE[1], Vijay K. SINGH[1,2], Juong G. RHEE[4], William E. JACKSON, III[1], Tzu-Cheg KAO[3] and Mark H. WHITNALL[1,*]

[1]Radiation Countermeasures Program, Armed Forces Radiobiology Research Institute, Uniformed Services University of the Health Sciences, 8901 Wisconsin Ave, Bethesda, MD 20889-5603, USA
[2]Department of Radiation Biology, F. Edward Hébert School of Medicine, Uniformed Services University of the Health Sciences, 8901 Wisconsin Ave, Bethesda, MD 20889-5603, USA
[3]Division of Epidemiology and Biostatistics, Department of Preventive Medicine and Biometrics, F. Edward Hébert School of Medicine, Uniformed Services University of the Health Sciences, 4301 Jones Bridge Road, Bethesda, MD 20814, USA
[4]Department of Radiation Oncology, University of Maryland School of Medicine, 655 West Baltimore St., Baltimore, MD 21201-1559, USA
*Corresponding author. Radiation Countermeasures Program, Armed Forces Radiobiology Research Institute, Uniformed Services University of the Health Sciences, 8901 Wisconsin Ave., Bethesda, MD 20889-5603. Phone: 1-301-295-9262; Fax: 1-301-295-6503; E-mail: mark.whitnall@usuhs.edu

(Received 12 April 2012; revised 25 June 2012; accepted 26 June 2012)

The steroid androst-5-ene-3ß,17ß-diol (5-androstenediol, 5-AED) elevates circulating granulocytes and platelets in animals and humans, and enhances survival during the acute radiation syndrome (ARS) in mice and non-human primates. 5-AED promotes survival of irradiated human hematopoietic progenitors *in vitro* through induction of Nuclear Factor-κB (NFκB)-dependent Granulocyte Colony-Stimulating Factor (G-CSF) expression, and causes elevations of circulating G-CSF and interleukin-6 (IL-6). However, the *in vivo* cellular and molecular effects of 5-AED are not well understood. The aim of this study was to investigate the mechanisms of action of 5-AED administered subcutaneously (s.c.) to mice 24 h before total body γ- or X-irradiation (TBI). We used neutralizing antibodies, flow cytometric functional assays of circulating innate immune cells, analysis of expression of genes related to cell cycle progression, DNA repair and apoptosis, and assessment of DNA strand breaks with halo-comet assays. Neutralization experiments indicated endogenous G-CSF but not IL-6 was involved in survival enhancement by 5-AED. In keeping with known effects of G-CSF on the innate immune system, s.c. 5-AED stimulated phagocytosis in circulating granulocytes and oxidative burst in monocytes. 5-AED induced expression of both *bax* and *bcl-2* in irradiated animals. *Cdkn1a* and *ddb1*, but not *gadd45a* expression, were upregulated by 5-AED in irradiated mice. S.c. 5-AED administration caused decreased DNA strand breaks in splenocytes from irradiated mice. Our results suggest 5-AED survival enhancement is G-CSF-dependent, and that it stimulates innate immune cell function and reduces radiation-induced DNA damage via induction of genes that modulate cell cycle progression and apoptosis.

INTRODUCTION

Because of the increasing threat posed by nuclear weapons [1], there is a pressing need for both (pre-irradiation) radioprotectants and (post-irradiation) therapeutics, as recognized by civilian and military government agencies [2–4]. 5-AED is being developed as a radioprotectant and therapeutic for ARS. The steroid induces resistance to a variety of infections in animals [5–10], enhances survival in mice and rhesus macaques exposed to whole-body γ-irradiation [11,

12], and induces hematopoiesis and hematopoietic growth factor expression [13, 14]. Its administration causes increases in circulating granulocytes, monocytes, NK cells and platelets in irradiated animals [14–16]. In humans, 5-AED induces elevations in circulating granulocytes and platelets, and exhibits minimal side effects [17]. 5-AED also displays beneficial effects after burn injury, trauma and sepsis [18–20]. A radiation countermeasure having a dose reduction factor (DRF) of 1.25 like 5-AED [15] would increase the radiation dose at which 50% of exposed personnel died by 25%. A mass casualty scenario could involve exposure of hundreds of thousands of people [21], and radiation dose-mortality curves are steep [22]. Hence a countermeasure with a DRF of 1.2–1.3 could reduce casualties by very large numbers. For example, in canines, supportive care (DRF 1.3) resulted in mortality falling from above 95% to below 5% at a radiation dose of 2.9 Gy [23].

Effects of 5-AED on hematopoiesis have been demonstrated by increases in granulocyte-macrophage colony-forming cells (GM-CFC) in mouse bone marrow after s.c. injections [15]. This has been correlated with increases in neutrophil progenitors in marrow as shown by histology [15]. We hypothesized that these effects were due to induction of hematopoietic growth factors and went on to show that s.c. administration of 5-AED caused increased serum concentrations of G-CSF in both unirradiated and irradiated mice [13]. The induction of G-CSF supported the hypothesis that 5-AED's survival-enhancing effects are due at least in part to stimulation of hematopoiesis, resulting in increased numbers of innate immune system cells in circulation. PCR analysis of hematopoietic tissues showed [24] that 5-AED administration was associated with elevation of mRNAs for Granulocyte-Monocyte-CSF, Interleukin (IL)-2, IL-3, IL-6 and IL-10 in spleen, and GM-CSF and IL-2 in bone marrow. The same study confirmed the 5-AED-stimulated increase in circulating G-CSF, and also showed enhancement by 5-AED of serum macrophage inflammatory protein-1γ (MIP-1 γ). A recent study found 5-AED strongly synergized with thrombopoietin at the level of immature hematopoietic progenitor cells in irradiated mice, whereas pegylated G-CSF amplified expansion of surviving progenitors [25].

A pharmacokinetic analysis of 5-AED in mice demonstrated that plasma 5-AED peaked 2 h after s.c. injection, remaining significantly above control after 4 days, but not 8 days. The time course of plasma 5-AED after buccal delivery (60 mg/kg) was similar, but levels were significantly lower compared to s.c. delivery. Plasma 5-AED 24 h after administration was not significantly different between s.c. and buccal delivery. However, whereas 5-AED enhanced survival when injected s.c. 24 h before irradiation, buccal 5-AED did not affect survival. Those results suggested that the survival-enhancing effects of 5-AED are dependent on events triggered during the first few hours after administration. We postulated these survival-enhancing early events involved induction of hematopoietic cytokines [15, 24]. However, this speculation was based on correlations, rather than a direct test of the hypothesis by blocking hematopoietic cytokines. In addition, the immediate target cells of 5-AED were not known.

To obtain more direct evidence regarding the mechanisms of 5-AED action, we tested the effects of 5-AED on irradiated human hematopoietic progenitor (CD34+) cells [26]. We found that 5-AED protected CD34+ cells from radiation damage, as shown by enhanced cell survival, clonogenicity, proliferation and differentiation. The data demonstrated that hematopoietic progenitor cells are direct targets of the steroid. Furthermore, 5-AED stabilized NFκB in irradiated cells and induced NFκB gene expression and activation [26]. NFκB is a transcription factor that induces genes that inhibit apoptosis, activate immune system cells and promote survival in irradiated cells [27–29]. An NFκB-binding region of the G-CSF promoter is required for induction of G-CSF by tumor necrosis factor-α and IL-1β in human embryonic lung (HEL) fibroblasts [30]. 5-AED stimulated release of G-CSF from human CD34+ cells, and this effect was blocked by the NFκB inhibitor N-benzoyloxycarbonyl (Z)-Leu-Leu-leucinal (MG132) [26]. Moreover, the survival-enhancing effects of 5-AED *in vitro* were dependent on both NFκB and G-CSF, as shown by siRNA inhibition of NFκB and neutralizing antibody blocking of G-CSF.

Given the results of the *in vitro* study [26], and the previous demonstration of 5-AED-induced G-CSF expression *in vivo* [13, 24], we wondered whether the survival enhancement by 5-AED in irradiated mice was dependent on G-CSF. Since our study of CD34+ cells only addressed one cell type, and effects of drugs in *in vitro* studies are often different from what is observed in whole animals, this required a direct test *in vivo*. We compared the effects of blocking G-CSF to blocking IL-6, since IL-6 is induced by 5-AED [24, 26], but was not necessary for the survival-enhancing effects of 5-AED *in vitro* [26]. Since the beneficial effects of 5-AED *in vitro* were dependent on NFκB and G-CSF, we also tested whether known effects of G-CSF and NFκB could be observed in irradiated animals after 5-AED administration. These effects include activation of innate immune system cells [28, 29, 31–38], modulation of radiation-responsive genes related to cell cycle progression, DNA repair, apoptosis [27] and protection against DNA damage [27].

MATERIALS AND METHODS

Animals

All studies were carried out in accordance with the principles and procedures of the National Research Council Guide for the Care and Use of Laboratory Animals [39]. All research was approved by the Institutional Animal Care

and Use Committee of the Armed Forces Radiobiology Research Institute (AFRRI). For antibody blocking studies, male CD2F1 mice were used (Harlan, Indianapolis, IN). For phagocytosis, oxidative burst and PCR studies, animals were male C3H/HeN mice (National Cancer Institute, Frederick, MD). For the comet assays, mice were male C3H/FeJ (Jackson Laboratory, Bar Harbor, Maine). Mouse strains were chosen according to the evolving standard practices of the laboratories performing the experiments. A body of work has shown that responses to 5-AED in various strains of mice, including B6D2F1/J [15, 16, 40], C3H [13, 24, 40] and CD2F1 [41], are quite similar. 5-AED is used routinely at AFRRI as a positive control in 30 day survival assays in CD2F1 mice when screening novel radiation countermeasure candidates (our unpublished data). The C3H/HeN and C3H/FeJ strains are closely related.

Mice were male, 6–8 weeks of age, 22–35 g body weight, and were held in quarantine for two weeks. Up to 8 mice were housed in sanitized 46 cm × 24 cm × 15 cm polycarbonate boxes with filter covers (MicroIsolator; Lab Products, Inc., Maywood, NJ) on autoclaved hardwood chip bedding in a facility accredited by the Association for the Assessment and Accreditation of Laboratory Animal Care International and were given feed and acidified (pH 2.5 – 3.0) water freely. The animal holding room was provided with conditioned fresh air that was changed at least 10 times per h. Air was kept at approximately 21°C and 50% (± 20%) relative humidity. The animal room was maintained on a 12-h light/dark full-spectrum lighting cycle. For each experiment, mice for all groups were selected from the same lot of animals (i.e. a cohort of mice delivered as a single item from the vendor, with the same birth date).

Injections

5-AED (androst-5-ene-3ß,17ß-diol, Steraloids, Wilton, NH), or vehicle (polyethylene glycol MW400, PEG-400, Sigma, St. Louis, MO) was injected s.c. in a volume of 0.1 ml, 24 h before irradiation. Neutralizing antibodies to G-CSF and IL-6 were used to determine the role of G-CSF and IL-6 on the survival of irradiated mice. CD2F1 mice received antibodies to either G-CSF or IL-6 (0.2 ml, 600 µg/mouse) or the appropriate isotype control antibody (0.2 ml, 600 µg/mouse) i.p. 16 h before irradiation. Monoclonal anti-mouse G-CSF and IL-6 antibodies, and rat IgG1 isotype control antibodies, were purchased from R&D Systems (R&D systems, Inc., Minneapolis, MN). Antibody was diluted to 3000 µg/ml in Dulbecco's phosphate-buffered saline (D-PBS) and administered in a volume of 0.2 ml. Neutralizing antibody experiments were repeated twice, $n = 16–20$ mice/group in each experiment. Group sizes for other experiments are shown in the figure legends.

Irradiations

For comet assays, mice were exposed to X-rays (250 kVp, 15 mA, 2 Gy/min) at the University of Maryland Medical Center in Baltimore, receiving midline doses of 1, 3 or 5 Gy. For all other experiments, mice were placed in ventilated Plexiglas containers and exposed bilaterally to γ-radiation from the AFRRI ^{60}Co source at 0.6 Gy/min. The radiation type (γ-rays or X-rays) was chosen based on the facilities of the laboratories performing the experiments. These γ-rays and X-rays were both low Linear Energy Transfer (LET) photons with similar energy profiles. Irradiations took place between 9 am and noon. Exposure time was adjusted so that animals received the midline tissue-absorbed doses described. Radiation dosimetry was based on the alanine/EPR (electron paramagnetic resonance) system [42, 43], currently accepted as one of the most accurate methods and used for intercomparison between national metrology institutions. The calibration curves used in dose measurements at AFRRI (spectrometer e-Scan, Burker Biospin, Inc., Madison, WI, USA) are based on standard alanine calibration sets purchased from the United States National Institute of Standards and Technology, Gaithersburg, MD, USA. The accuracy of the constructed calibration curve was additionally verified by intercomparison with the National Physical Laboratory of the United Kingdom. The dose rate was measured using small tissue-equivalent alanine pellets in the cores of mouse phantoms positioned in the compartments of the mouse rack. Optically stimulated luminescence (InLight system from Landauer, Inc., Glenwood, IL, USA), traditional ionization chambers, and new generation Gafchromic film colorimetry were used as supporting and quality-control methods.

Phagocytosis and oxidative burst assays

For assays of phagocytosis, the reagents and instructions from Phagotest® kits (Orpegen Pharma, Heidelberg, Germany) were used. Heparanized blood was incubated with FITC-labeled opsonized E. coli at 37°C. Negative control samples were incubated on ice. FITC fluorescence of surface-bound bacteria was quenched at the end of the incubation. Bacteria were discriminated from blood cells with a DNA label and appropriate gating during acquisition and analysis. Data are presented as percentage of granulocytes or monocytes having performed phagocytosis (i.e. positive for FITC labeling).

For assays of oxidative burst, the reagents and instructions from BurstTest® kits (Orpegen Pharma, Heidelberg, Germany) were used. The experimental design was similar to that for phagocytosis, except that heparanized blood was incubated with opsonized unlabeled bacteria, and then incubated with dihydrorhodamine 123, which is converted to rhodamine 123 and trapped in cells in the presence of reactive oxidants. Negative control samples were not incubated

with bacteria. Samples were then analyzed in the flow cytometer. Data are presented as percentage of granulocytes or monocytes having produced detectable reactive oxygen species (i.e. positive for rhodamine 123 labeling).

In both assays, granulocytes and monocytes were distinguished on the basis of forward light scatter (size) and side scatter (granularity). These experiments were repeated twice.

Gene expression

RNA isolation procedures

Mice were anesthetized to unconsciousness with Isoflurane (Abbott Laboratories, Chicago, IL) before blood was collected from the abdominal vena cava with a 23-gauge needle. Anesthetized mice were humanely euthanized by cervical dislocation after blood collection. Spleens were harvested after euthanization. Whole spleen from each mouse was homogenized in 1.0 ml RNA STAT-60 (Tel-Test Inc., Friendswood, TX) in a polytron homogenizer (Brinkmann Instruments, Inc., Westbury, NY). Homogenized splenic suspension was immediately frozen and kept at –70°C until further use. Total RNA of each sample was extracted according to the RNA STAT-60 manufacturer's protocol. Total RNA was isolated by homogenization in TRIzol reagent (Life Technologies, Gaithersburg, MD) followed by QIAGEN® RNeasy® 96 Universal Tissue Kits (Qiagen, Chatsworth, CA). The concentration and quality of total RNA were determined with the Agilent 2100 bioanalyzer with nanochips (Agilent Technologies, Palo Alto CA), spectrophotometrically (260 nm/280nm ratio), and agarose gel electrophoresis.

QRT-PCR assays

Total RNA was converted to complementary DNA (cDNA) by a reverse transcription step with M-MLV reverse transcriptase, OligodT primer, RNase inhibitor and dNTPs. For PCR amplification, a maximum of 20 ng of cDNA was used per 50 µL PCR reaction. PCR amplifications were performed using the iCycler iQ Sequence Detection System (Bio-Rad Laboratories, Hercules CA) on 96-well microtiter plates with optical caps. Reactions were performed in a total volume of 50 µL containing 20 ng cDNA. Real-time RT-PCR assays were carried out using 1× buffer (10× PCR buffer is 200 mM Tris-HCl, pH 8.4, 500 mM KCl). SYBR Green primer pair validation experiments were carried out in 50 µl using Taq (0.025 U/µl reaction volume), 5 µl of a 1/10000 SYBR Green dilution, 300 nM of each PCR primer, 1× buffer, dNTPs (200 µM), and 3.5 mM MgCl2. PCR was performed to determine levels of mRNA coding for *gadd45a, ddb1, ddb2, cdkn1a, bax* and *bcl-2*, as well as 18S rRNA subunit which was used as an internal control. All cDNA samples were amplified for 40–50 cycles using denaturation at 94°C for 30 s, annealing and extension at 60°C for 60 s. The ratio of fluorescence intensity of target-specific product to that of the internal control product represents relative levels of target mRNA expression. The performance of primers and probe sets included in our multiplex qRT-PCRs was evaluated using serial dilutions (one-fifth or one-tenth dilutions) of murine cDNA spanning three orders of magnitude. All components were maintained under universal conditions. PCR amplifications were always performed in duplicate or triplicate wells, using universal temperature cycles: 10 min at 94°C, followed by 35–45 two-temperature cycles (15 s at 94°C and 1 min at 60°C).

Primers and probes

Amplicon lengths were set between 70 and 110 bp. To avoid co-amplification of contaminating genomic DNA, primers were (where possible) designed on different exons or intron–exon boundaries. All primers and hydrolysis probe sequences were designed with Primer Express software. The primers were synthesized by Loftstrand Laboratories (Gaithersburg MD). Selected fluorophores were FAM (6-carbonylfluorescein) and TexasRed™. Appropriate Black Hole dark quenchers were matched for each fluorophore. Gene expression was measured in five mice per group.

Halo-Comet assay

Mice were injected s.c. with 5-AED at different doses (10, 30 and 100 mg/kg), and exposed to X-rays (1, 3 or 5 Gy at 2 Gy/min) 24 h later. Within 2 min after irradiation, spleens were excised and minced to separate splenocytes. These cells were washed once and suspended in ice-cold PBS (5×10^5 cells/ml). For the halo-comet assay, a filter paper was punched with 5 mm diameter holes, placed on a clean glass slide, and moistened with PBS. The cell suspension in PBS was mixed with the same volume of a pre-warmed 2% agarose solution (60°C), and a drop of the mixture (41° C) was applied to the hole of a filter paper. In order to remove lipids and proteins, the gel in a filter paper was exposed to an NN (0.03 M NaOH and 1 M NaC1) lysis solution for 60 min at 4°C, followed by washing with an NE (0.03 M NaOH and 2 mM EDTA) solution for 30 min at 4° C. This treated gel was transferred to a submarine gel apparatus (E-C Apparatus Corp.), and DNA separation was achieved by applying 16.5 DC volts for 6 min (3 volts/cm, 18 mA) to the NE solution. After electrophoresis, the gel was washed with water for 15 min, and then stained with 2.5 µg/ml propidium iodide (PI) for 10 min, in a dark box. The PI intercalated to the DNA strands was excited at 545 nm (BP-545), and the red fluorescence emission at 580 nm was observed under an epi-fluorescent microscope (Olympus BH-2) with the aid of a 590 nm barrier filter. The red fluorescence light (DNA image) was enhanced with the Dark-Invader night vision system (Meyers & Co. Inc., Redmond, WA), and was either digitized with a frame grabber or recorded on a videotape for later analysis. To quantify DNA damage, individual comet images were

analyzed with Accuware (Automatic Visual Inspection, Santa Clara, CA). The length of the halo-comet image corresponded to the extent of DNA damage [44]. The analysis was repeated for 300 nuclei for each group.

Statistical analysis

All results were expressed as means ± SE. For antibody neutralization experiments, survival data were analyzed using Fishers Exact Test adjusted for multiple comparisons using Bonferroni correction. Phagocytosis and oxidative burst data were analyzed by ANOVA. PCR data were analyzed in terms of relative gene expression. The cycle number at which the fluorescent signal of a given reaction well crossed the threshold value was denoted as the threshold cycle (C_T). Target data from each well were normalized to the internal standard, 18S ribosomal subunit, using the formula ΔC_T = target C_T – internal standard C_T. Radiation effects on gene expression levels were analyzed further by comparison to a reference standard (i.e. vehicle calibrator; nonirradiated sham-treated samples). Microsoft Excel-fitted lines were obtained using standard regression analysis programs within Excel XP (Microsoft Corporation, Redmond, WA) and Sigma Plot 5.0 (SPSS Inc., Chicago, IL). Standard errors of C_T were determined for each value. Analysis of variance (ANOVA) was used to detect significant differences among groups at each time point. If there was any significant difference among the groups, the Tukey-Kramer method was used for pair-wise comparisons. For comet assays, least square means were adjusted for multiple comparisons using Tukey-Kramer. Differences were considered significant if the two-sided P value was <0.05. A software package, PC SAS, was used for statistical analyses.

RESULTS

Effects of neutralization of G-CSF or IL-6 on survival of 5-AED-treated, irradiated mice

Mice were exposed to TBI at a dose (9.25 Gy, 0.6 Gy/min) that resulted in 30-day survival of 44% in controls (drug vehicle and isotype antibody injections, Fig. 1). Survival of vehicle-treated irradiated mice after pre-treatment with neutralizing antibody (anti-G-CSF, 0% or anti-IL-6, 25%) was not significantly different from survival after vehicle and isotype control antibody. When irradiated mice were pre-treated with 5-AED and isotype control antibody, all animals survived. Isotype control antibody injections had no effect on survival of unirradiated mice receiving vehicle or 5-AED injections (not shown). However, as shown in Fig. 1, when irradiated mice were injected with neutralizing antibody to G-CSF, the survival-enhancing effect of 5-AED was blocked (31% survival, compared to 100% with isotype control antibody). Survival in these mice was not significantly different from mice receiving vehicle plus isotype control (44%) or vehicle plus anti-G-CSF (0%). On the other hand, pre-treatment of irradiated mice with neutralizing antibody to IL-6 had no effect on the ability of 5-AED to enhance survival: all mice in this group survived (Fig. 1). The results indicate endogenous G-CSF but not IL-6 was involved in survival enhancement by 5-AED.

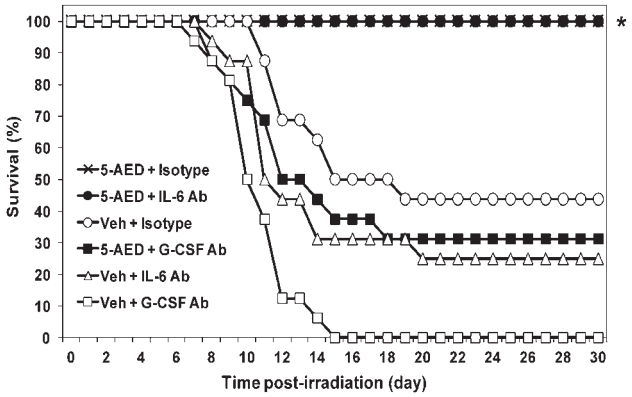

Fig. 1. Effects of neutralizing anti-G-CSF or anti-IL-6 antibody on survival of irradiated mice. 5-AED or vehicle was injected s.c. 24 h before total body γ-irradiation (9.25 Gy). Antibodies were injected i.p. 16 h before irradiation. *$P < 0.05$ compared to vehicle, for both 5-AED + isotype control antibody and 5-AED + anti-IL-6 antibody. Results from one of two experiments showing similar results; $n = 16$–20 mice/group in each experiment.

Phagocytosis and oxidative burst in innate immune cells in irradiated mice

Phagocytosis of opsonized FITC-labeled bacteria was measured using flow cytometry of granulocytes and monocytes in blood taken from sublethally irradiated or sham-irradiated mice that had been injected s.c. with 5-AED or vehicle 24 h before irradiation (3 Gy) or sham-irradiation (Fig. 2). The radiation dose was relatively low in this experiment to allow sufficient numbers of circulating cells to study. A decrease in phagocytic activity was observed in both granulocytes and monocytes 1 day after irradiation (Fig. 2). ANOVA revealed a significant effect of 5-AED on phagocytic activity in granulocytes 1 day after irradiation and 4 days after sham-irradiation (Fig. 2). However, no effect of 5-AED on phagocytosis was observed in monocytes (Fig. 2).

To measure oxidative burst, we analyzed baseline activity in granulocytes and monocytes (i.e. in the absence of incubation with bacteria), and the effect of incubation with opsonized unlabeled bacteria (Fig. 3). In contrast to phagocytosis, which was stimulated by 5-AED in granulocytes but not monocytes (Fig. 2), oxidative activity was stimulated by 5-AED in monocytes but not granulocytes (Fig. 3). In monocytes, both baseline and bacteria-stimulated oxidative activity were higher in 5-AED-treated mice 1 and 4 days

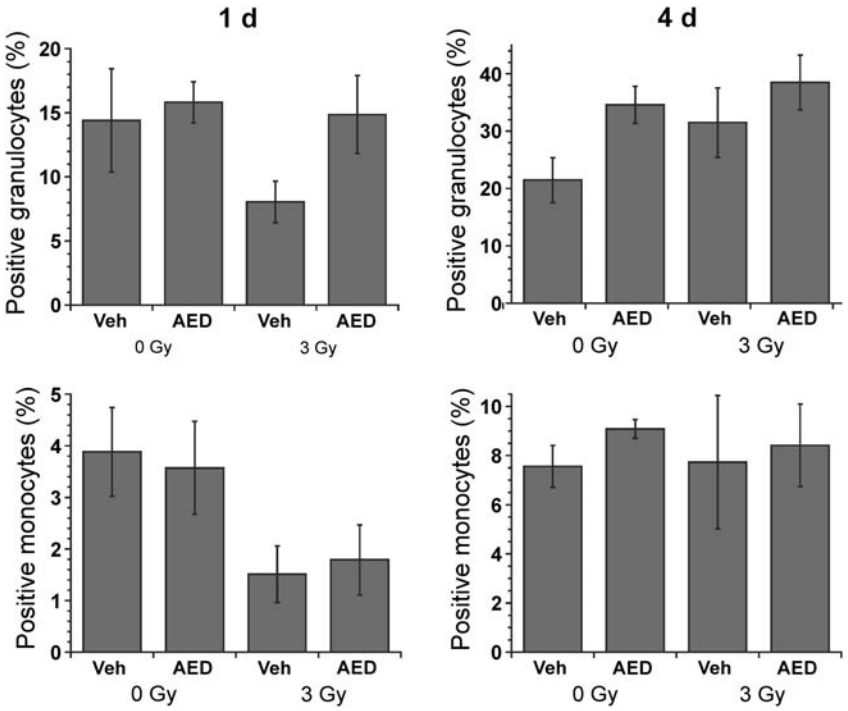

Fig. 2. Effects of 5-AED on phagocytosis in circulating granulocytes and monocytes. Injections of 5-AED (160 mg/kg) 24 h before sham-irradiation (0 Gy) or total body γ-irradiation (3 Gy) caused increases in phagocytotic activity in granulocytes ($P < 0.05$) as measured by flow cytometry. Blood was incubated with FITC-labeled opsonized *E. coli* at 37°C. Negative control samples were incubated on ice. $n = 18–20$ mice/group.

after sham-irradiation or irradiation (Fig. 3). In summary, s.c. 5-AED stimulated phagocytosis in circulating granulocytes and oxidative burst in monocytes.

Expression of genes related to cell cycle progression, DNA repair and apoptosis

5-AED was administered s.c. (30 mg/kg) 24 h prior to irradiation at a high sublethal dose (7.5 Gy) and spleens were collected 4 h after 5-AED injection, or 4 or 24 h after irradiation. The results presented in Fig. 4 show modulation of messages of apoptotic genes by 5-AED in irradiated and sham-irradiated mice: 5-AED induced pro-apoptotic *bax* expression 4 h after sham-irradiation and irradiation. Decreased expression of anti-apoptotic *bcl-2* was observed 4 h after 5-AED injection, as compared to vehicle-treated mice (Fig. 4, not significant). However, 5-AED pre-treatment 24 h before irradiation enhanced *bcl-2* expression when compared to down-regulated vehicle-treated controls 4 h post-irradiation (Fig. 4). The results show increased levels of message for both *bax* and *bcl-2* gene expression in spleen tissue after 5-AED injection. No significant change in the *bax/bcl-2* ratio was observed.

5-AED administration resulted in no change in transcription levels of the regulator of cell cycle progression and DNA repair, *cdkn1a*, in spleens of sham-irradiated mice (Fig. 5). However, the steroid induced a rise in *cdkn1a* mRNA 4 h post-irradiation (Fig. 5).

Ddb1, which is not up-regulated in response to radiation in human or mouse models, is up-regulated in response to 5-AED treatment. DDB1 and DDB2 form a heterodimer involved in DNA repair. 5-AED induced significant increases in *ddb1* expression in two groups as shown in Fig. 6: 4 h post-irradiation, and 24 h after sham irradiation. Treatment with 5-AED had no significant effect on the radiation-responsive DNA repair genes *gadd45a* and *ddb2* in splenocytes (data not shown). The results of the gene regulation study in spleen tissue show 5-AED-induced modulation of genes that that regulate apoptosis, with no clear indication of a shift in the balance of pro-apoptotic vs anti-apoptotic genes. However, there was a significant induction of some but not all genes involved in regulation of cell proliferation and DNA repair (*cdkn1a* and *ddb1*).

Effects of radiation on whole blood gene expression biomarkers

Changes in relative gene expression in whole blood are shown in Table 1. mRNA for *cdkn1a* measured in whole blood 24 h post-irradiation displayed an increase (fold change) of 6.6 ± 0.4. Expression of *bcl-2* decreased 0.68 ± 0.1 fold, and *bax* increased 1.9 ± 0.6 fold. Expression of the DNA repair gene *gadd45a* increased 25.0 ± 15 fold. As was found for splenocytes, *ddb2* transcription values in whole blood remained unchanged.

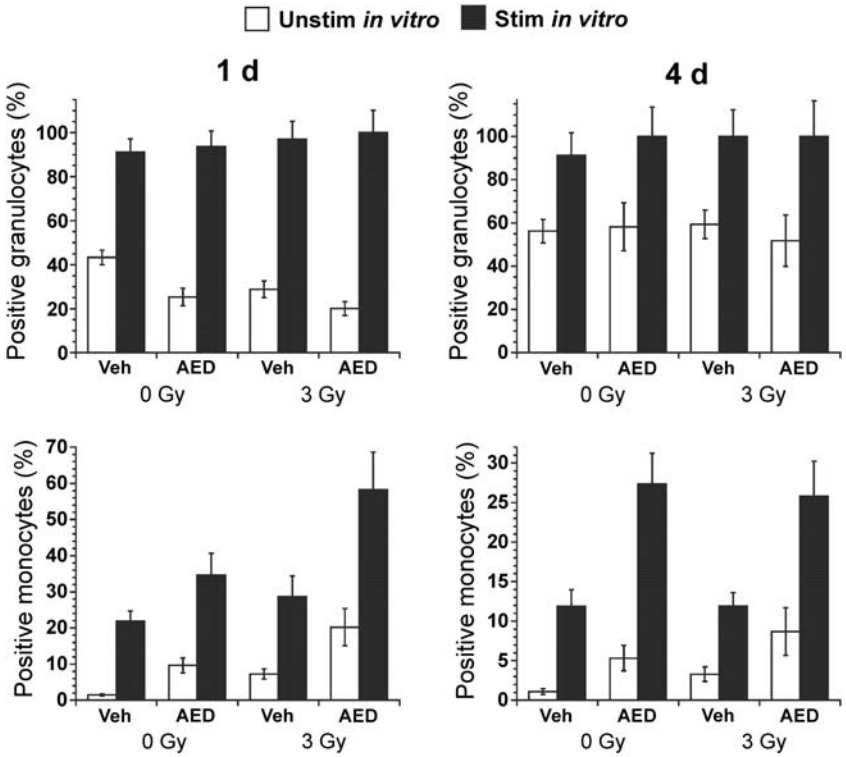

Fig. 3. Effects of s.c. 5-AED on oxidative burst in circulating granulocytes and monocytes. Injections of AED (160 mg/kg) caused increases in oxidative activity in monocytes when injected 24 h before sham-irradiation (0 Gy) or total body γ-irradiation (3 Gy) ($P < 0.001$) as measured by flow cytometry. Radiation induced an increase in monocyte baseline oxidative activity (in the absence of bacterial stimulation) ($P < 0.05$). The experimental design was similar to that for phagocytosis (Fig. 2), except that blood was incubated with opsonized unlabeled bacteria, and then incubated with dihydrorhodamine 123, which is converted to rhodamine 123 and trapped in cells in the presence of reactive oxidants. Negative control samples were not incubated with bacteria. $n = 18–20$ mice/group.

Effects of 5-AED pre-treatment on DNA damage in splenocytes of irradiated mice

Following treatment with X-rays (1–5 Gy) alone, the halo-comet image length increased with increasing doses of X-rays (Fig. 7), suggesting dose-dependent DNA damage. When mice were treated with 5-AED 24 h before irradiation, the image length was significantly shorter than what was obtained with vehicle pre-treatment, indicating a protective effect of 5-AED. All tested doses of 5-AED (10, 30 and 100 mg/kg) produced the same protective effect (Fig. 7). The data indicate 5-AED injected 24 h before irradiation reduced radiation-induced DNA damage measured immediately after irradiation.

DISCUSSION

Roles of cytokines in survival-enhancing effects of 5-AED

Previous reports showed administration of 5-AED induces G-CSF expression in mice and in cultured human hematopoietic progenitor cells [13, 26], and that the survival-enhancing effects of 5-AED on hematopoietic progenitor cells *in vitro* were dependent on G-CSF. Since G-CSF promotes survival in irradiated mice [45], canines [46] and NHP [47], and is recommended for use in human radiation casualties [2], we tested whether the survival-enhancing effects of 5-AED *in vivo* were dependent on G-CSF using neutralizing antibodies. Our results are consistent with studies documenting the essential role of endogenous G-CSF in the mechanism of action of some other radiation countermeasures [48, 49]. We also tested the role of IL-6, since administration of 5-AED induces IL-6 expression in mice and in cultured human hematopoietic progenitor cells [24, 26], and anti-IL-6 antibody reduces the radioprotective effects of IL-1 and TNF in mice [50]. However, in our previous *in vitro* study, the survival-enhancing effects of 5-AED on hematopoietic progenitor cells *in vitro* were not dependent on IL-6 [26]. Consistent with the *in vitro* results, blocking IL-6 did not inhibit the radioprotective effects of 5-AED *in vivo*.

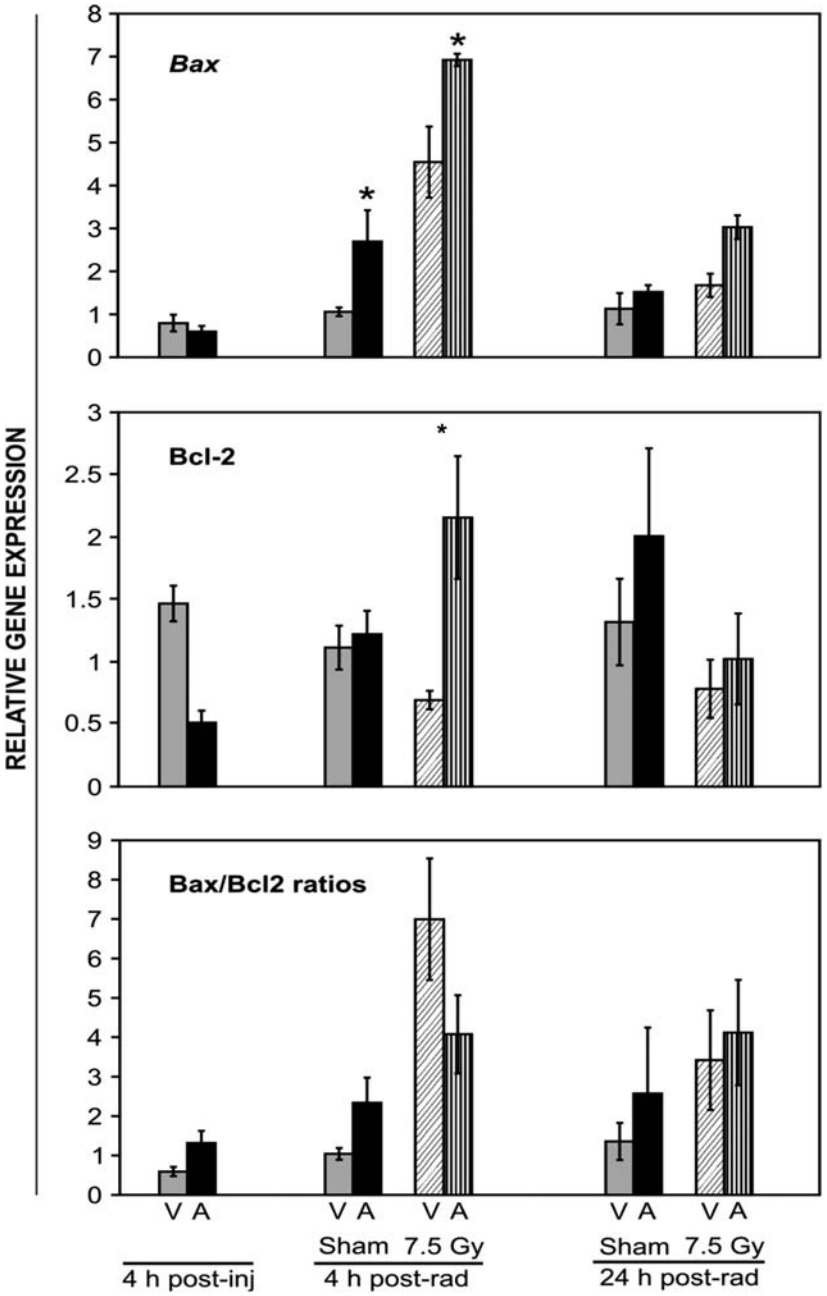

Fig. 4. Quantitation of *bax, bcl2* and *bax/bcl2* ratio mRNA by QRT-PCR in spleens of 5-AED-treated and irradiated mice. Six- to eight-week old C3H/HeN mice received s.c. injections of 5-AED (30 mg/kg) 24 h before 7.5 Gy γ-irradiation. Spleens were collected 4, 28 or 48 h after steroid administration. V = vehicle, A = 5-AED, Means ± SEM, $*P < 0.05$, 5-AED-treated vs vehicle-treated. $n = 10$ mice for all groups except 4 h post-vehicle, which contained 5 mice.

Effects of 5-AED on innate immune cell function

G-CSF is induced by the pro-survival transcription factor NFκB [30], and the 5-AED-induced G-CSF we observed in human hematopoietic progenitor cells was NFκB-dependent [26]. Increased levels of G-CSF and/or NFκB after 5-AED administration to mice could enhance survival by reducing apoptosis in hematopoietic progenitor cells [51]. However, G-CSF also induces activation of cells of the innate immune system, as shown by gene microarray analysis [31]. Functional assays show G-CSF upregulates phagocytosis in neutrophils, with conflicting results on upregulation of oxidative burst [32–37]. Inhibition of

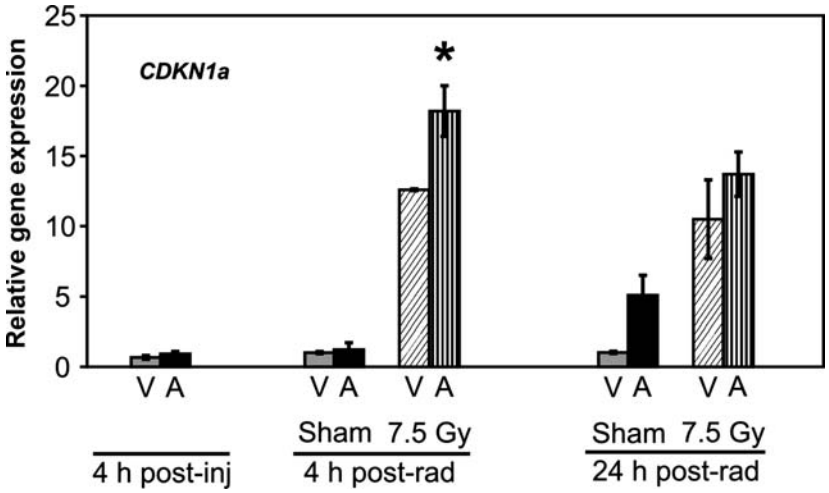

Fig. 5. Quantitation of *cdkn1a* mRNA by QRT-PCR in splenocytes of 5-AED-treated and irradiated mice. Six- to eight-week-old C3H/HeN mice received s.c. injections of 5-AED (30 mg/kg) 24 h before 7.5 Gy γ-irradiation. Samples were collected 4, 28 or 48 h after steroid administration. V = vehicle, A = 5-AED, Means ± SEM, $*P < 0.05$, 5-AED-treated vs vehicle-treated. $n = 10$ mice for all groups except 4 h post-vehicle, which contained 5 mice.

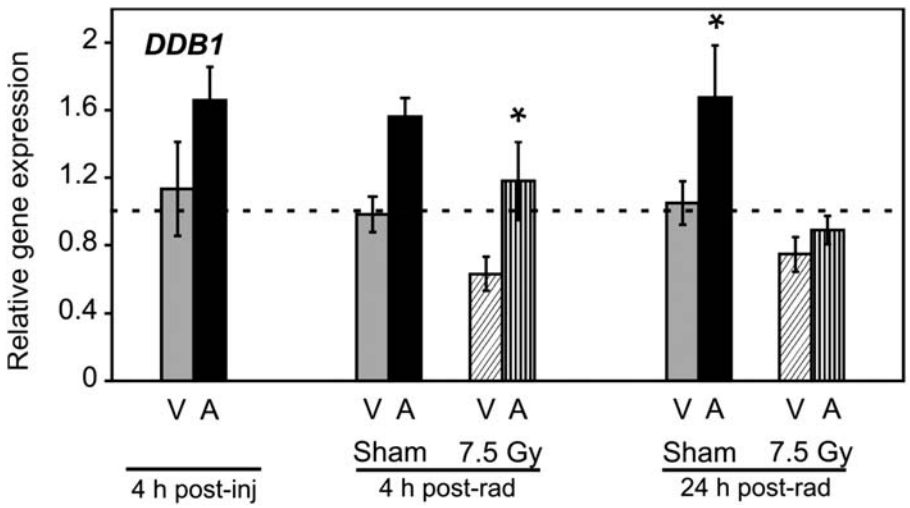

Fig. 6. Quantitation of *ddb1* RNA by QRT-PCR in splenocytes of 5-AED-treated and irradiated mice. Six- to eight-week-old C3H/HeN mice received s.c. injections of 5-AED (30 mg/kg) 24 h before 7.5 Gy γ-irradiation. Samples were collected 4, 28 or 48 h after steroid administration. V = vehicle, A = 5-AED, Means ± SEM $*P < 0.05$, 5-AED-treated vs vehicle-treated. $n = 10$ mice for all groups except 4 h post-vehicle, which contained 5 mice.

NFκB decreased neutrophil phagocytosis and microbicidal capacity [38]. A large variety of NFκB target genes is activated in stimulated monocytes/macrophages, including G-CSF and inducible nitric oxide synthase, which contributes to the oxidative burst [28]. Hence it has been postulated that NFκB plays a central role in coordinately controlling gene expression during monocyte/macrophage activation [28]. Since 5-AED induces both G-CSF and NFκB in human hematopoietic progenitor cells, we hypothesized that the radioprotective efficacy of 5-AED *in vivo* may be due partially to activation of innate immune cells by G-CSF and/or NFκB. Our finding that 5-AED administration to mice increased phagocytotic activity of circulating granulocytes and oxidative activity in circulating monocytes supports this hypothesis. The data support our hypothesis [16] that survival enhancement by 5-AED in irradiated animals could be due, at least in part, to increased effectiveness by innate immune cells at removing harmful

Table 1. Average gene expression changes in blood of five mice 24 h post-irradiation (7.5 Gy)

Accession no.	Symbol; Name	Relative Gene Expression
Cell cycle/proliferation		
AY655697	CDKN1A; cyclin-dependent kinase inhibitor 1A (p21)	(+) 6.6 ± 0.4
Apoptosis		
NM_009741	BCL2	(−) 0.68 ± 0.1
NM_007527	BAX; BCL2-associated X protein	(+) 1.9 + 0.6
DNA repair		
BC011141	GADD45A; growth arrest and DNA-damage-inducible ***	(+) 25.0 ± 15.0
AY027937	DDB2	0.0 ± 0.0

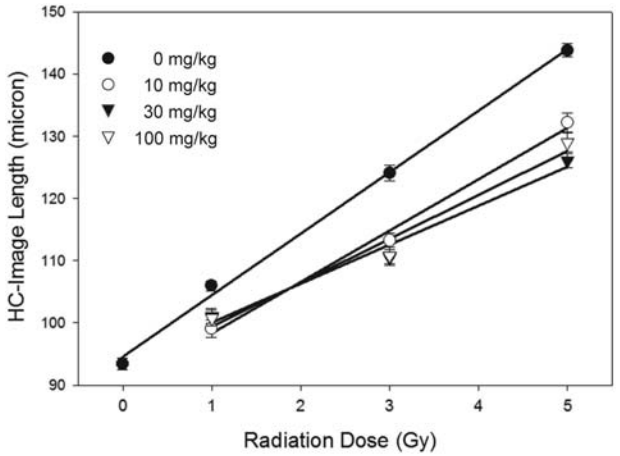

Fig. 7. Quantification of halo-comet assay results in mouse splenocytes 2 min after X-irradiation. 5-AED was injected s.c. 24 h before whole-body irradiation at 10 mg/kg, 30 mg/kg and 100 mg/kg. Halo-comet lengths for each of the three doses were significantly lower than for vehicle controls ($P < 0.05$). There were no statistical differences between results for the different 5-AED doses, except at 5 Gy: halo-comet lengths for 30 mg/kg were significantly shorter than for 10 mg/kg. $n = 6$ mice/group.

microorganisms, supplementing the effect of increased numbers of circulating innate immune cells.

The striking dichotomy between granulocytes and monocytes in terms of which function (phagocytosis vs oxidative burst) was stimulated by 5-AED is intriguing. Further experimentation will be necessary to determine how 5-AED affects the different intracellular signaling pathways that regulate these two functions [52]. Granulocytes (mainly neutrophils) play an important role in the inflammatory response [53]. Since inflammation is thought to be a major component of radiation injury [54], the lack of stimulation of oxidative burst in granulocytes by 5-AED may serve to prevent the steroid from aggravating this component of radiation injury. In fact, 5-AED has been shown to inhibit inflammation [19, 55, 56]. Moreover, nonoxidative killing is an important function of both neutrophils and monocytes [57].

Monocytes also participate in inflammation, but they are far fewer in number, so the 5-AED-induced increase in monocyte oxidative burst may not be a major factor in aggravating inflammation. 5-AED inhibits inflammatory responses in brain monocytes (microglia) [58]. However, stimulation of the monocyte oxidative burst by 5-AED would facilitate killing of microorganisms by these cells. The 5-AED-induced increase in oxidative activity in monocytes with no modulation of phagocytotic ability may indicate a stimulation of extracellular killing by these cells [59]. The increase in oxidative activity in monocytes of 5-AED-treated mice may be due to induced differentiation of these cells, since G-CSF is known to cause differentiation of monocytes [60].

Effects of 5-AED on gene expression in splenocytes

The balance between apoptosis and survival/proliferation after irradiation is largely controlled by the Ataxia Telangiectasia Mutated (ATM) protein, which activates pro-survival factor NF-κB and pro-apoptotic P53 [51]. The balance between pro-survival and pro-apoptotic pathways regulated by these signals determines whether cells will survive, enter into a state of cell cycle arrest, or undergo apoptosis. P53 is a transcription factor that induces a G1 or G2 arrest via activation of *cdkn1a* (*p21*), creating extra time for DNA repair mechanisms and impeding apoptosis [61–64]. If DNA fails to repair, P53 initiates apoptosis by activation of members of the pro-apoptotic members of the *bax/bcl-2* family [65–67]. We found increased levels of message for both *bax* and *bcl-2* gene expression after 5-AED injection, which did not provide a clear signal as to whether 5-AED was promoting or inhibiting apoptosis. This may be due to the heterogeneous population of cells in the spleen, with different cell types responding differently to radiation and 5-AED.

Expression of mRNA for the cell cycle control gene *cdkn1a* is used as an indicator of growth arrest, which facilitates DNA repair [68]. The clear increase in expression of *cdkn1a* after 5-AED administration indicates that the overall effect of the steroid on splenocytes was to promote cell cycle arrest in G1 and G2, which would be consistent with protection against apoptosis. However, the relationship between *cdkn1a* and apoptosis is complex. Inhibition of apoptosis is one outcome of overexpression of *cdkn1a*, but senescence would be another since radiation-triggered accelerated senescence is dependent on CDKN1A function [69]. CDKN1A was found to be pro-apoptotic in 32Dc13 murine myeloblasts induced to differentiate into

granulocytes by removal of IL-3 and addition of G-CSF [70]. The same group found that CDKN1A inhibited granulocytic differentiation in 32Dc13 cells [71]. It remains to be seen whether similar effects occur *in vivo*, in the absence of IL-3 deprivation. Some of the protective effect of 5-AED against DNA damage may be mediated by CDKN1A's promotion of chromosomal stability [72].

We observed significant up-regulation of *ddb-1* gene expression 4 h post-irradiation in the 5-AED treatment group, but no change was observed for the radiation-responsive DNA repair genes *ddb-2* and *gadd45a* [73, 74]. This is worthy of note because *gadd45a* mRNA is a global indicator of cellular stress. To our knowledge, this is the first time a compound has been reported to alter *ddb-1* gene expression. Depletion of DDB1 protein is known to result in increased DSB in widely dispersed regions throughout the genome as evidenced by γH2AX foci formation and activation of ATM and ATR damage response pathways [75].

Current evidence suggests that DDB1 is involved in general cellular responses to DNA damage. DDB1 protein is a component of the Cullin4A ubiquitin ligase and is involved in DNA repair, cell cycle regulation, DNA replication, and maintenance of genome integrity [75]. DDB1/DDB2 complexes are known to recognize some UV-damaged DNA lesions, and initiate the nucleotide excision repair process [76, 77]. Although the mechanism is not yet known, it appears that DDB assists in nucleotide excision repair in chromatin. Using mouse models, Cang *et al.* [78] showed that *ddb1* is required for embryogenesis, and the conditional inactivation of *ddb1* results in the apoptosis of proliferating cells owing to the accumulation of cell cycle regulators and genomic instability. Cang *et al.* [79] also reported that tissue-specific deletion of *ddb1* in mouse epidermis led to dramatic accumulation of CDKN1A, arrest of cell cycle at G2/M, and selective apoptosis in mouse skin. Upregulation of *ddb1* by 5-AED but not by radiation exposure suggests an important effect of 5-AED is to maintain genome integrity after radiation exposure. This hypothesis is supported by the direct observation of reduced DNA damage in splenocytes of 5-AED-treated mice in the comet assay.

Effects of 5-AED on gene expression in whole blood

5-AED-induced changes in whole blood were similar to splenocytes for *cdkn1a*, *bax* and *ddb2* after irradiation, were in the opposite direction for *bcl2* post-irradiation, and *gadd45a* was induced strongly in whole blood but not in splenocytes. The results indicate an overall effect on circulating cells of promoting DNA repair and preserving genome integrity (*cdkn1a*, *ddb2* and *gadd45a*). However, whereas the regulation of genes in the spleen indicated both pro-apoptotic and anti-apoptotic influences of 5-AED, the effect on whole blood was clearly pro-apoptotic. This effect of 5-AED may be related to removal of defective cells from circulation. The pro-apoptotic effect of 5-AED on whole blood does not interfere with its stimulation of increases in numbers of circulating innate immune cells [15, 16]. It also does not seem to be related to lymphocytes, since 5-AED administration is not associated with changes in numbers of lymphocytes [15, 16].

CONCLUSION

DNA damage elicits a multifaceted response that includes cell cycle arrest, transcriptional activation of DNA repair genes, and apoptosis. We demonstrate that in mouse spleen, DNA damage leads to induction of specific alterations in gene expression patterns. The expression of genes involved in cell cycle control, repair of DSBs, and apoptosis were modulated after treatment with 5-AED. These results are consistent with our comet assay results showing decreased DNA damage shortly after irradiation of 5-AED-pretreated mice. The present findings indicate that the survival-enhancing effects of 5-AED are dependent on endogenous G-CSF and are associated with functional activation of innate immune cells. Further studies are required to elucidate the exact mode of radioprotection at the molecular level, including a better understanding of the relative rates of proliferation and apoptosis in conjunction with DNA damage signaling, persistence of DNA damage versus transient DNA damage, and underlying molecular mechanisms involved in the radiation response.

FUNDING

This work was supported by the Armed Forces Radiobiology Research Institute (RAB4AO to M.B.G., RAB2AX to V.K.S. and RAB2AD to M.H.W.) and the National Institute of Allergy and Infectious Diseases (Y1–AI–3809–01 to M.H.W.)

ACKNOWLEDGEMENTS

The authors acknowledge the excellent technical support of Christopher McLeland, Vaishali Parekh and Cynthia Inal; the staffs of the AFRRI Veterinary Sciences and Radiation Sources Departments; Cheng-Min Chang for preparation of high quality RNA samples; and Patrice Bolte for graphic services. The views expressed here are those of the authors; no endorsement by the US Department of Defense or any US Government agency has been given and should not be inferred.

REFERENCES

1. Allison G. Nuclear disorder: surveying atomic threats. *Foreign Affairs* 2010;**89**:74–85.

2. Waselenko JK, MacVittie TJ, Blakely WF *et al*. Medical management of the acute radiation syndrome: recommendations of the Strategic National Stockpile Radiation Working Group. *Ann Intern Med* 2004;**140**:1037–51.
3. Pellmar TC, Rockwell S. Priority list of research areas for radiological nuclear threat countermeasures. *Radiat Res* 2005;**163**:115–23.
4. Department of Defense Chemical and Biological Defense Program. *Annual Report to Congress*. Washington, DC: Department of Defense, 2010.
5. Carr DJ. Increased levels of IFN-gamma in the trigeminal ganglion correlate with protection against HSV-1-induced encephalitis following subcutaneous administration with androstenediol. *J Neuroimmunol* 1998;**89**:160–7.
6. Daigle J, Carr DJ. Androstenediol antagonizes herpes simplex virus type 1-induced encephalitis through the augmentation of type I IFN production. *J Immunol* 1998;**160**:3060–6.
7. Hernandez-Pando R, De La Luz Streber M, Orozco H *et al*. The effects of androstenediol and dehydroepiandrosterone on the course and cytokine profile of tuberculosis in BALB/c mice. *Immunology* 1998;**95**:234–41.
8. Loria RM, Padgett DA. Androstenediol regulates systemic resistance against lethal infections in mice. *Arch Virol* 1992;**127**:103–15.
9. Padgett DA, Loria RM, Sheridan JF. Endocrine regulation of the immune response to influenza virus infection with a metabolite of DHEA-androstenediol. *J Neuroimmunol* 1997;**78**:203–11.
10. Padgett DA, Sheridan JF, Loria RM. Steroid hormone regulation of a polyclonal TH2 immune response. *Ann N Y Acad Sci* 1995;**774**:323–25.
11. Whitnall MH, Villa V, Seed TM *et al*. Molecular specificity of 5-androstenediol as a systemic radioprotectant in mice. *Immunopharmacol Immunotoxicol* 2005;**27**:15–32.
12. Stickney DR, Dowding C, Authier S *et al*. 5-androstenediol improves survival in clinically unsupported rhesus monkeys with radiation-induced myelosuppression. *Int Immunopharmacol* 2007;**7**:500–5.
13. Singh VK, Shafran RL, Inal CE *et al*. Effects of whole-body gamma irradiation and 5-androstenediol administration on serum G-CSF. *Immunopharmacol Immunotoxicol* 2005;**27**:521–34.
14. Stickney DR, Dowding C, Garsd A *et al*. 5-androstenediol stimulates multilineage hematopoiesis in rhesus monkeys with radiation-induced myelosuppression. *Int Immunopharmacol* 2006;**6**:1706–13.
15. Whitnall MH, Elliott TB, Harding RA *et al*. Androstenediol stimulates myelopoiesis and enhances resistance to infection in gamma-irradiated mice. *Int J Immunopharmacol* 2000;**22**:1–14.
16. Whitnall MH, Inal CE, Jackson WE, III *et al*. *In vivo* radioprotection by 5-androstenediol: Stimulation of the innate immune system. *Radiat Res* 2001;**156**:283–93.
17. Stickney DR, Groothuis JR, Ahlem C *et al*. Preliminary clinical findings on NEUMUNE as a potential treatment for acute radiation syndrome. *J Radiol Prot* 2010;**30**:687–98.
18. Araneo B, Daynes R. Dehydroepiandrosterone functions as more than an antiglucocorticoid in preserving immunocompetence after thermal injury. *Endocrinology* 1995;**136**:393–401.
19. Szalay L, Shimizu T, Suzuki T *et al*. Androstenediol administration after trauma-hemorrhage attenuates inflammatory response, reduces organ damage, and improves survival following sepsis. *Am J Physiol Gastrointest Liver Physiol* 2006;**291**:G260–6.
20. Shimizu T, Szalay L, Hsieh YC *et al*. A role of PPAR-gamma in androstenediol-mediated salutary effects on cardiac function following trauma-hemorrhage. *Ann Surg* 2006;**244**:131–8.
21. Swartz HM, Flood AB, Gougelet RM *et al*. A critical assessment of biodosimetry methods for large-scale incidents. *Health Phys* 2010;**98**:95–108.
22. Anno GH, Young RW, Bloom RM *et al*. Dose response relationships for acute ionizing-radiation lethality. *Health Phys* 2003;**84**:565–75.
23. MacVittie TJ, III, Farese AM, Jackson W, III. Defining the full therapeutic potential of recombinant growth factors in the post radiation-accident environment: the effect of supportive care plus administration of G-CSF. *Health Phys* 2005;**89**:546–55.
24. Singh VK, Grace MB, Jacobsen KO *et al*. Administration of 5-androstenediol to mice: pharmacokinetics and cytokine gene expression. *Exp Mol Pathol* 2008;**84**:178–88.
25. Aerts-Kaya FS, Visser TP, Arshad S *et al*. (5 Jun 2012) 5-Androstene-3b,17b-diol promotes recovery of immature hematopoietic cells following myelosuppressive radiation and synergizes with thrombopoietin. *Int J Radiat Oncol Biol Phys,* [http://dx.doi.org/10.1016/j.ijrobp.2012.04.021].
26. Xiao M, Inal CE, Parekh VI *et al*. 5-Androstenediol promotes survival of gamma-irradiated human hematopoietic progenitors through induction of nuclear factor-kappaB activation and granulocyte colony-stimulating factor expression. *Mol Pharmacol* 2007;**72**:370–9.
27. Ahmed KM, Li JJ. NF-kappa B-mediated adaptive resistance to ionizing radiation. *Free Radic Biol Med* 2008;**44**:1–13.
28. Baeuerle PA, Henkel T. Function and activation of NF-kappa B in the immune system. *Annu Rev Immunol* 1994;**12**:141–79.
29. Pahl HL. Activators and target genes of Rel/NF-kappaB transcription factors. *Oncogene* 1999;**18**:6853–66.
30. Dunn SM, Coles LS, Lang RK *et al*. Requirement for nuclear factor (NF)-kappa B 65 and NF-interleukin-6 binding elements in the tumor necrosis factor response region of the granulocyte colony-stimulating factor promoter. *Blood* 1994;**83**:2469–79.
31. Buzzeo MP, Yang J, Casella G *et al*. Hematopoietic stem cell mobilization with G-CSF induces innate inflammation yet suppresses adaptive immune gene expression as revealed by microarray analysis. *Exp Hematol* 2007;**35**:1456–65.
32. Mitchell GB, Albright BN, Caswell JL. Effect of interleukin-8 and granulocyte colony-stimulating factor on priming and activation of bovine neutrophils. *Infect Immun* 2003;**71**:1643–9.
33. Ohkubo T, Tsuda M, Suzuki S *et al*. Peripheral blood neutrophils of germ-free rats modified by in vivo granulocyte-colony-stimulating factor and exposure to natural environment. *Scand J Immunol* 1999;**49**:73–7.
34. Carulli G. Effects of recombinant human granulocyte colony-stimulating factor administration on neutrophil phenotype and functions. *Haematologica* 1997;**82**:606–16.

35. Hoglund M, Hakansson L, Venge P. Effects of in vivo administration of G-CSF on neutrophil functions in healthy volunteers. *Eur J Haematol* 1997;**58**:195–202.
36. Meyer CN, Nielsen H. Priming of neutrophil and monocyte activation in human immunodeficiency virus infection. Comparison of granulocyte colony-stimulating factor, granulocyte-macrophage colony-stimulating factor and interferon-gamma. *APMIS* 1996;**104**:640–6.
37. Sullivan GW, Carper HT, Mandell GL. The effect of three human recombinant hematopoietic growth factors (granulocyte-macrophage colony-stimulating factor, granulocyte colony-stimulating factor, and interleukin-3) on phagocyte oxidative activity. *Blood* 1993;**81**:1863–70.
38. Giraldo E, Martin-Cordero L, Hinchado MD *et al*. Role of phosphatidylinositol-3-kinase (PI3K), extracellular signal-regulated kinase (ERK) and nuclear transcription factor kappa beta (NF-k βτα) on neutrophil phagocytic process of Candida albicans. *Mol Cell Biochem* 2010;**333**:115–20.
39. National Research Council of the National Academy of Sciences. *Guide for the Care and Use of Laboratory Animals*, 8th edn. Washington, DC: National Academies Press, 2011.
40. Whitnall MH, Wilhelmsen CL, McKinney L *et al*. Radioprotective efficacy and acute toxicity of 5-androstenediol after subcutaneous or oral administration in mice. *Immunopharmacol Immunotoxicol* 2002;**24**:595–626.
41. Whitnall MH, Elliott TB, Landauer MR *et al*. Protection against gamma-irradiation with 5-androstenediol. *Mil Med* 2002;**167**:64–5.
42. Nagy VY, Desrosiers MF. Complex time dependence of the EPR signal of irradiated L-alpha-alanine. *Appl Radiat Isot* 1996;**47**:789–93.
43. Nagy V. Accuracy considerations in EPR dosimetry. *Appl Radiat Isot* 2000;**52**:1039–50.
44. Rhee JG, Liu J, Suntharalingam M. Halo-comet assay. In: Reeves GI, Jarrett DG, Seed TM *et al*. (eds). *Triage of Irradiated Personnel: Appendix D*. Bethesda, MD: Armed Forces Radiobiology Research Institute, 1996;D5–9.
45. Patchen ML, MacVittie TJ, Solberg BD *et al*. Therapeutic administration of recombinant human granulocyte colony-stimulating factor accelerates hemopoietic regeneration and enhances survival in a murine model of radiation-induced myelosuppression. *Int J Cell Cloning* 1990;**8**:107–22.
46. MacVittie TJ, Monroy RL, Patchen ML *et al*. Therapeutic use of recombinant human G-CSF (rhG-CSF) in a canine model of sublethal and lethal whole-body irradiation. *Int J Radiat Biol* 1990;**57**:723–36.
47. Farese AM, Cohen MV, Gibbs AM *et al*. Filgrastim administration significantly improves survival in nonhuman primates following a 50% lethal dose of total body irradiation. Abstracts, 55th Annual Meeting of the Radiation Research Society 2009;**2009**:127.
48. Singh VK, Brown DS, Kao TC. Alpha-tocopherol succinate protects mice from gamma-radiation by induction of granulocyte-colony stimulating factor. *Int J Radiat Biol* 2010;**86**:12–21.
49. Kalechman Y, Zuloff A, Albeck M *et al*. Role of endogenous cytokines secretion in radioprotection conferred by the immunomodulator ammonium trichloro(dioxyethylene-0-0)tellurate. *Blood* 1995;**85**:1555–61.
50. Neta R, Perlstein R, Vogel SN *et al*. Role of interleukin 6 (IL-6) in protection from lethal irradiation and in endocrine responses to IL-1 and tumor necrosis factor. *J Exp Med* 1992;**175**:689–94.
51. Xiao M, Whitnall MH. Pharmacological countermeasures for the acute radiation syndrome. *Curr Mol Pharmacol* 2009;**2**:122–33.
52. Dai X, Jayapal M, Tay HK *et al*. Differential signal transduction, membrane trafficking, and immune effector functions mediated by FcgammaRI versus FcgammaRIIa. *Blood* 2009;**114**:318–27.
53. Heasman SJ, Giles KM, Ward C *et al*. Glucocorticoid-mediated regulation of granulocyte apoptosis and macrophage phagocytosis of apoptotic cells: implications for the resolution of inflammation. *J Endocrinol* 2003;**178**:29–36.
54. Wang J, Hauer-Jensen M. Neuroimmune interactions: potential target for mitigating or treating intestinal radiationinjury. *Br J Radiol* 2007;**80** Spec No 1:S41–8.
55. Rontzsch A, Thoss K, Petrow PK *et al*. Amelioration of murine antigen-induced arthritis by dehydroepiandrosterone (DHEA). *Inflamm Res* 2004;**53**:189–98.
56. Auci D, Nicoletti F, Mangano K *et al*. Anti-inflammatory and immune regulatory properties of 5-androsten-3beta, 17beta-diol (HE2100), and synthetic analogue HE3204: implications for treatment of autoimmune diseases. *Ann N Y Acad Sci* 2005;**1051**:730–42.
57. Pinheiro da Silva F, Machado MC. (1 Jun 2012) Antimicrobial peptides: Clinical relevance and therapeutic implications. *Peptides*, [http://dx.doi.org/10.1016/j.peptides.2012.05.014].
58. Saijo K, Collier JG, Li AC *et al*. An ADIOL-ERbeta-CtBP transrepression pathway negatively regulates microglia-mediated inflammation. *Cell* 2011;**145**:584–95.
59. Chow OA, von Kockritz-Blickwede M, Bright AT *et al*. Statins enhance formation of phagocyte extracellular traps. *Cell Host Microbe* 2010;**8**:445–54.
60. Jiang D, Schwarz H. Regulation of granulocyte and macrophage populations of murine bone marrow cells by G-CSF and CD137 protein. *PLoS ONE* 2010;**5**:e15565.
61. Wendt J, Radetzki S, von Haefen C *et al*. Induction of p21CIP/WAF-1 and G2 arrest by ionizing irradiation impedes caspase-3-mediated apoptosis in human carcinoma cells. *Oncogene* 2006;**25**:972–80.
62. Dotto GP. p21(WAF1/Cip1): more than a break to the cell cycle? *Biochim Biophys Acta* 2000;**1471**:M43–56.
63. Szymczyk KH, Shapiro IM, Adams CS. Ionizing radiation sensitizes bone cells to apoptosis. *Bone* 2004;**34**:148–56.
64. Verheyde J, de Saint-Georges L, Leyns L *et al*. The role of Trp53 in the transcriptional response to ionizing radiation in the developing brain. *DNA Res* 2006;**13**:65–75.
65. Cenni B, Aebi S, Nehme A *et al*. Epidermal growth factor enhances cisplatin-induced apoptosis by a caspase 3 independent pathway. *Cancer Chemother Pharmacol* 2001;**47**:397–403.
66. Berk AJ. Recent lessons in gene expression, cell cycle control, and cell biology from adenovirus. *Oncogene* 2005;**24**:7673–85.

67. Crowe DL, Sinha UK. p53 apoptotic response to DNA damage dependent on bcl2 but not bax in head and neck squamous cell carcinoma lines. *Head Neck* 2006;**28**:15–23.
68. Li MJ, Wang WW, Chen SW *et al*. Radiation dose effect of DNA repair-related gene expression in mouse white blood cells. *Med Sci Monit* 2011;**17**:BR290–7.
69. Mirzayans R, Scott A, Cameron M *et al.* Induction of accelerated senescence by gamma radiation in human solid tumor-derived cell lines expressing wild-type TP53. *Radiat Res* 2005;**163**:53–62.
70. Ghanem L, Steinman R. A proapoptotic function of p21 in differentiating granulocytes. *Leuk Res* 2005;**29**:1315–23.
71. Ghanem L, Steinman RA. 21Waf1 inhibits granulocytic differentiation of 32Dcl3 cells. *Leuk Res* 2006;**30**:1285–92.
72. Duensing A, Ghanem L, Steinman RA *et al*. 21(Waf1/Cip1) deficiency stimulates centriole overduplication. *Cell Cycle* 2006;**5**:2899–902.
73. Amundson SA, Grace MB, McLeland CB *et al*. Human in vivo radiation-induced biomarkers: gene expression changes in radiotherapy patients. *Cancer Res* 2004;**64**:6368–71.
74. Grace MB, McLeland CB, Gagliardi SJ *et al*. Development and assessment of a quantitative reverse transcription-PCR assay for simultaneous measurement of four amplicons. *Clin Chem* 2003;**49**:1467–75.
75. Lovejoy CA, Lock K, Yenamandra A *et al*. DDB1 maintains genome integrity through regulation of Cdt1. *Mol Cell Biol* 2006;**26**:7977–90.
76. Tang J, Chu G. Xeroderma pigmentosum complementation group E and UV-damaged DNA-binding protein. *DNA Repair (Amst)* 2002;**1**:601–16.
77. Cong F, Tang J, Hwang BJ *et al*. Interaction between UV-damaged DNA binding activity proteins and the c-Abl tyrosine kinase. *J Biol Chem* 2002;**277**:34870–8.
78. Cang Y, Zhang J, Nicholas SA *et al.* Deletion of DDB1 in mouse brain and lens leads to p53–dependent elimination of proliferating cells. *Cell* 2006;**127**:929–40.
79. Cang Y, Zhang J, Nicholas SA *et al*. DDB1 is essential for genomic stability in developing epidermis. *Proc Natl Acad Sci USA* 2007;**104**:2733–7.